Manipulating the Size and Morphology of Aluminum Hydrous Oxide Nanoparticles by Soft-Chemistry Approaches

H. Y. Zhu,[a *] X. P. Gao,[b] D. Y. Song,[b] Simon P. Ringer,[a] Y. X. Xi,[c]

[a] *Australian Key Centre for Microanalysis & Microscopy and School of Chemistry, The University of Sydney, NSW 2006, Australia*
[b] *Institute of New Energy Material Chemistry, Nankai University, Tianjin 300071, China*
[c] *Faculty of Science, Xian Jiaotong University, Xian 710049, China*

Published as:

Zhu, Huaiyong and Gao, Xueping and Song, Deying and Ringer, Simon and Xi, Yingxin and Frost, Ray (2005) Manipulating the size and morphology of aluminum hydrous oxide nanoparticles by soft-chemistry approaches. *Microporous and Mesoporous materials* 85:pp. 226-233.

* Corresponding author, Dr H. Y. Zhu
e-mail: h.zhu@emu.usyd.edu.au, ,

Abstract

We demonstrate control of the size and morphology of aluminum hydrate nanoparticles synthesized by a hydrothermal reaction through manipulating pH value of the reaction mixture, hydrothermal temperature and the surfactant used. Porous laths formed under acidic conditions, while the lath-width increased with temperature and single-crystal porous laths were formed. At neutral or high pH values, porous plates of several nanometers thick were obtained. The pore sizes on both laths and plates were ~2-3 nm. Stringy lath-shaped nanoparticles were obtained with polyethylene glycol surfactant. It demonstrates that we can precisely control nanoparticle size and morphology using soft chemical methods. Furthermore, these nanoparticles transformed to γ-alumina nanocrystallites after heating to 673K, and retained the morphology of the parent boehmite. We provide a detailed characterization of the nanoparticulates and discuss the mechanism of their formation and subsequent transformation.

Key words: nanoparticles, hydrothermal synthesis, pore plates, boehmite, γ-alumina, morphology, surfactant, micelles.

Introduction

γ-alumina is one of the most important oxides, attracting much attention for years because of their potential for broad applications in advanced catalysts, adsorbents, composite materials and ceramics [1-5]. In recent years, γ-alumina-particles with nanoscale dimensions and morphological specificity have attracted enormous interest from both fundamental and practical viewpoints [5-26] Since the properties, surface and crystal structure of nanoparticles are size-dependent [14, 27] these fine nanostructures have potential to exhibit unusual properties. Various γ-alumina nanostructures have been synthesized, such as mesoporous alumina molecular sieves [7-9, 14] nanofibers [10-12, 16, 19, 20, 23] and nanotubes [17, 18] "Soft chemistry" approaches are emerging as a powerful method for the synthesis of delicate alumina nanostructures, which often involves the use of surfactants and boehmite (AlOOH) as intermediate products [10, 11, 13-17] The γ-alumina can be obtained from boehmite by a simple dehydration process at a temperature above 673K. During heating, the boehmite nanostructures undergo an isomorphous transformation to nanocrystalline γ-alumina, and this product γ-alumina can retain the morphology of the parent boehmite nanostructures [10, 17, 18, 20, 23] Therefore, one can synthesize delicate structures of boehmite through hydrothermal processing and subsequently transform them into γ-alumina by heating. Because of the moderate conditions and a number of tunable experimental parameters in these soft-chemistry processes, it is possible to achieve a variety of nanostructures that are difficult or impossible to achieve by other means. As illustrated in the literature [10,11,13-17,23] there is indeed considerable parameter-space available for tuning so as to create a specific nanostructures via the hydrothermal reactions since different regimes of reaction mechanism become operational. Variations in the structures at the nanoscale can have significant impact on the properties of the final product alumina and open up new applications-opportunities [4-6, 10, 12-14, 20]. On the other hand, the synthesis of nanostructures of boehmite and γ-aluminas in aqueous systems is not only of great interest in materials research, but may also explain the existence of aluminum oxide nanoparticles in nature, where the conditions for soft chemistry processes are often found. We reported recently that boehmite nanofibers can be formed from a precipitate of aluminum hydrous oxide in the presence of poly(ethylene oxide) (PEO) surfactant at

373K [10]. The boehmite nanofibers grow rapidly when fresh precipitate of aluminum hydrate was supplied at regular intervals [23] The formation and growth processes were conducted at the same temperature (373K), pH (6-8) and use of the same PEO surfactant.

In this paper, we describe the importance of the experimental parameters, hydrothermal temperature and pH value and explore the role of another surfactant (polyethylene glycol). We report a rich diversity in morphology and size of the boehmite nanoparticles with control of these experimental parameters, alone or in combination and demonstrate the utility of soft chemistry methods for creating new boehmite nanostructures such as porous nanolaths and porous nanoplates.

Materials and Methods

Materials Analytical grade $NaAlO_2$ and acetic acid, from Aldrich, were used to prepare the aluminum hydrate precipitate. Nonionic polyethylene oxide (PEO) surfactant, Tergitol 15S-7 from Aldrich, was used in this study. This PEO surfactant has a general chemical formula $C_{12\text{-}14}H_{25\text{-}29}O(CH_2CH_2O)_7H$, and average molecular weights of about 508.

Preparation. Aluminum hydrate precipitate was prepared by dropping 50 ml of $NaAlO_2$ solution containing 18.8 g of $NaAlO_2$·(0.2 mole of Al) into 50 ml of 5N acetic acid solution while stirring vigorously. The white precipitate was recovered by centrifugation and washed with water 4 times to remove the sodium ions. 40 gram of the surfactant was mixed with the washed aluminium hydrate cake. The sticky mixture is stirred for at least 1 hour and then transfered into a closed autoclave and kept in an oven at a designed temperature between 373 and 473 K for two days. The mixture contains about 0.2 mole of $Al(OH)_3$ and ~50 g of H_2O. The autogenous pressures in the closed autoclave at 373K and 473, are about 101 and 1550 kPa, respectively.

To examine the influence of pH of the reaction mixture, we used acetic acid solution to lower the pH of the washed aluminum hydrate precipitate from 6 - 8 to 2 - 4, and ammonia solution to increase the pH to ≥ 9, prior to the autoclaving. The autoclaved wet cake samples were dried in air at 373 K and the dried solids were then calcined at 773 K for 20 h to produce the γ-alumina nanostructures. The heating temperature was raised at rate of 2 K/min, starting from 373 K. To examine the influence of surfactant structure in such synthesis, polyethylene glycol (PEG) surfactant $HO(CH_2CH_2O)_{8\text{-}9}H$ was used, instead of PEO, and all other parameters were kept unchanged.

Characterisation. X-ray diffraction (XRD) patterns of the sample powder were recorded on a Shimadzu XRD-6000 diffractometer equipped with a graphite monochromator. Cu *K*α radiation (0.15418 nm) and a fixed power source (40 kV, 40 mA) were used. The data was collected at a scanning rate of 0.2º/min over the 2θ range of 2 to 90º. Transmission electron microscopy (TEM) images were taken with a Philips CM12 operating at 120 kV on powder samples deposited onto a copper mesh-grid coated with holey carbon film. High-resolution transmission electron microscopy (HRTEM) images were taken on a JEOL JEM-3000F field emission electron microscope under an accelerating voltage of 300 kV. N_2 adsorption/desorption isotherms were measured at liquid nitrogen temperature (77.3K), using a gas sorption analyzer (Quantachrome, Autosorb-1). The samples were degassed at 523 K in a vacuum below 10^{-3} Torr for 16 h prior to the measurement. The specific surface area was calculated by

the BET equation [28], using the data in a P/P_0 range between 0.05 and 0.2; the pore size distribution of the derived using method in reference [29].

Results and Discussion

The experimental parameters of the hydrothermal treatments influence greatly the form of the boehmite nanostructures. The morphological and crystal features of the nanostructured particles are highly dependent upon the treatment temperature, the pH value of the reaction mixtures and the surfactant existing in the reaction mixture. The effects of these major experimental parameters are examined.

Effect of Temperature. TEM images in Figure 1 illustrate the influence of the hydrothermal temperature on the morphologies of boehmite nanoparticulates obtained from the acidic reaction mixtures (pH<4). At 373K thin nanofibers were obtained; they are about 3 nm thick and 30 to 60 nm long (Figure 1a), similar to the fibers prepared at neutral mixture (pH 6 - 8) [10, 23]. These fibers are, in terms of crystal phases, a mixture of boehmite with an orthorhombic structure (JCPDS #83-2384) and bayerite with a monoclinic structure (JCPDS #83-2256) as shown Figure 2a. In this figure the diffraction peaks of boehmite and bayerite are labeled with b and c, respectively.

(Figures 1 and 2)

The product from hydrothermal treatments at 423 K was laths about 6 nm wide and length between 30 and 70 nm (Fig. 1b). Aluminum acetate (peaks labeled with letter a in Figure 2a) was found to be an important phase co-existing with boehmite phase according to its XRD pattern. These laths possessed a row of pores 2-3 nm in size, which is similar to the dimension of an individual micelle of PEO surfactant [30-33]. In a polarized media, the ethylene oxide groups of the surfactant head toward the outside of the micelles while the hydrocarbon chain (of 12 – 14 carbon atoms) will tend to diffuse inside, forming rod-like micelles of about a few nanometer thick. The surfactant micelles interact with the hydroxyl group on the surface of boehmite particles through hydrogen bonding [8, 10] It is noted in previous studies that the rod-shape micelles could direct the boehmite nanofiber growth through this bonding [10, 23].

The pore size distribution of this sample is derived from N_2 adsorption data [29] and provided in Figure 3. There is a peak at about 2.5 nm in the PSD, indicating a considerable amount of pores with a diameter of 2.5 nm in the samples. They are the pores on the laths, which are observed in images of Figure 1b and 1d. It seems that some surfactant micelles were encapsulated in the boehmite matrix during the synthesis because the pore size is in a similar dimension to the thickness of the rod-like micelles. The walls of the pores are thin boehmite crystals. In some case, the walls between pores in one lath do not exist so that slit-like rings are observed (Figure 1d). These boehmite laths could be transformed to γ-alumina nanocrystallites by a heating at 723 K, but retained the morphology of the parent boehmite. This phenomenon was observed for boehmite fibers [10]. Figure 4 is the image of the γ-alumina porous laths obtained form the boehmite nanolaths in Figure 1b.

(Figures 3 and 4)

Further raising of the temperature of the hydrothermal treatment results in increase in the lath width. The solid obtained at 473K is wide porous laths (Figure 1d) of

pure boehmite phase. Aluminum acetate was not observed in the diffraction patterns of the product (Figure 2a) because it is unstable at higher temperature. The sample shown in Fig. 1c was obtained at 473K (pH<4). The aspect ratio of the laths decreased from ~ 10 at 373 K to ~ 6 at 473 K. Meanwhile, these wide laths have more than one row of pores. It appears that as the temperature increases, the nanoparticles tend to join together in parallel (side by side). The diffraction peaks in the XRD pattern of the boehmite product obtained at 473 K are sharper (Figure 2a), compared with the corresponding peaks of the products obtained at 423 K, indicating a larger crystal size in the solid obtained at higher temperature. It has also been found that the plot of ln *W* versus the reciprocal of the treatment temperature (1/*T*) is linear (Figure 5), where *W* is the width of the 1D-particulates (fibers and laths).

(Figure 5)

Because the reaction period for the products is two days, *W* can also be regarded as the growth rate of the 1D-particulates in the direction of width (width increase in two day) so that the plot in Figure 5 is an approximation of the relationship between growth rate and reaction temperature. The improvement in crystallinity of the boehmite nanoparticles reveals that the Ostwald ripening process, in which larger crystallites grow at the expense of dissolving smaller crystallites driven by a reduction in surface energy, is involved in such a structural evolution because the Ostwald ripening mechanism generally leads to increase in the average crystal size. The linear relation of Figure 5 supports that the growth in the width is due to Ostwald ripening process because a linear relation is usually observed for such a process. Hydrothermal treatment at high temperatures (e.g. above 423K) leads to significant improvement in the crystallinity of the product. Above 453 K, the porous laths are single crystal grains of boehmite, as shown in the HRTEM images (Figure 6). The porous laths (Figure 6a) and plates (Figure 6b) obtained at 473K, but pH <4 and pH >9, respectively, are single crystal particles of boehmite with pores of 2-3 nm on them. Thus we conclude that as the temperature increases, the boehmite crystallinity is obviously improved regardless of the pH of the reaction mixtures.

(Figure 6)

The high hydrothermal treatment temperature also leads to another interesting feature in the particle morphology: most of the porous laths prepared at 473K have two sharp ends (Figure 7). This shape formation is due to the fastest growth rate in the *a*-axis <100> direction [34]. In this regime, the particulates grow at different rates from direction to another resulting in a shape of two opposite sharp ends. However, such growth impedes elongation by assembly along this direction. In a previous study on the growth of boehmite nanofibers, fresh aluminum hydrate precipitate was added at regular interval to initial mixture of boehmite and polyethylene oxide (PEO) surfactant to yield longer fibers [23]. The same growth process for reaction spanning 2-8 days was also conducted at a higher temperature of 423 K, but wide porous nanolaths rather than long fibers were obtained. Obviously, a process at lower temperature is preferred if long fibers are required. This conclusion is consistent with the fact that one-dimensional structures of boehmite reported in literatures, such as fibers and tubes [10, 11, 17-20, 23]

are synthesized at a hydrothermal temperature of 423K or below, unless the synthesis carried out in reaction systems of low aluminum content [4, 5].

(Figure 7)

Effect of pH. As the temperature increases, the influence of pH is progressing more important. From a neutral or a basic reaction mixture, we obtained thin plates that are several nanometers thick and tens of nanometers in lateral dimensions (Figure 6b and Figure 8). Similarly, there are the pores of about 2-3 nm in size on these plates. Comparing the aspect ratio of the particles obtained at 473K, we find that as the pH of the reaction mixture increases the aspect ratio decreases. The product from acidic mixture (pH <4) is porous laths, and it is porous plate from a basic mixture (pH <9). While the product obtained at pH ~ 6 is a mixture of the laths and plate (Figure 8). In a neutral or high pH environment, the thin fibers that we observed at a lower temperature of 373 K [10, 23] appear unstable at high temperatures and have a strong tendency to connect together side by side forming porous plates. Generally, the thin fibers have over 400 m^2/g of specific surface area as calculated from nitrogen sorption data [10] and are in a metastable state due to high surface energy. These fibers are stabilized by the surfactant micelles through hydrogen bonding [10, 11, 23]. The specific surface area of the porous plate samples was about 100 m^2/g, and with a much smaller specific surface area, these plates are more stable. On the other hand, in the reaction mixture of high pH, there are substantial amounts of negatively charged species, such as $[Al(OH)_6]^{3-}$ and polymerized hydrate oxide $[Al_nO_m(OH)_p]^{(p+2m-3n)-}$. This is especially true at high temperatures because of increases in the solubility of these species. These species can be incorporated into the boehmite lattice, leading to growth in the direction of the particle width. Actually, in the system without surfactant, the particle morphology of boehmite is very sensitive to the pH of the reaction system. We can only obtain fibers from a reaction system of a pH about 5. In the reaction with PEO surfatant, the influence of the pH on the particle morphology appears gradually as the hydrothermal treatment temperature is raised. The two experimental parameters can jointly affect the morphology and structure of the nanoparticles.

Effect of surfactant. The surfactant plays a crucial role in the formation of the boehmite nanostructures [8-11, 25]. The surfactant, or surfactant micelles formed in a polarized media, interact with the hydroxyl group on the surface of boehmite particles through hydrogen bonding, and thus affect the morphology of the product boehmite nanoparticles [8, 10, 23]. Therefore, adding different surfactants in the synthesis could lead to boehmite nanoparticles of different structures. When polyethylene glycol (PEG) surfactant $HO(CH_2CH_2O)_{8-9}H$ was used, instead of PEO, and all other parameters were kept unchanged, we obtained stringy lath-shaped nanoparticles (Figure 9). Without a hydrocarbon chain, the PEG molecules are more hydrophilic and spread readily along on boehmite particle surface due to hydrogen bonding. This is different from that the PEO surfactant, which exist in the reaction system as rod-like micelles. This is thought to be the major reason for the formation of the stringy lath without pores on them. Such a structure allows maximizing the number of the hydrogen bonding between the surfactant and particle surface and thus achieve a state of the lowest system energy. Interestingly, the thickness of these laths is about 3 nm, which is the same as the thickness of the nanofibers. However, these laths are much longer, up to 200-300 nm. The stacking of

needle-like crystals of dimensions about 3 × 3 × 10 nm has been reported for boehmite crystallites formed from the hydrolysis of an aluminum compound [35]. We believe that crystal domains of ~3 nm thick are the building units to form thin and long laths in the presence of the PEG surfactant, because this configuration allows the maximum amount hydrogen bonding between the oxygen atom of the $-CH_2CH_2O-$ units and the hydroxyl groups on the boehmite surface.

(Figure 9)

Manipulating the size and morphology of the nanocrystallites in the presence of surfactants [10, 11, 36] is intrinsically similar to the biomineralisation process in which organic molecules exert a remarkable level of control over the assembly of nanocrystalline mineral phases into complex structures [37]. This highlights the great prospect of biomimic synthesis of inorganic nanostructures and may provide clues in explaining the existence of aluminum oxide nanoparticles in nature.

Summary

In the approach yielding boehmite nanoparticles from the aluminium hydrate precipitate in the presence of the surfactants, the morphological and crystal features of aluminum hydrate products are highly dependent upon the synthesis conditions: hydrothermal temperature, the acidity of the reaction mixtures and type of surfactant. Therefore, we could tailor the morphology and crystalline of the nanoparticulates by manipulating the temperature, pH and surfactants. Fibers, thin and wide laths with pores and porous plate can be achieved. This work highlights a useful synthesis strategy for low temperature, aqueous syntheses of metal oxide nanomaterials with tailorable structural specificity such as size, morphology and crystal structure. One can synthesize delicate nanostructures of metal hydrous oxides via wet chemical reactions and converted them into oxide structures by an isomorphous transformation (dehydration) at elevated temperatures. For instance, the γ-alumina nanoparticles can be obtained from the boehmite nanostructures and used to develop advanced catalysts, catalyst supports, ceramics and composite materials. Moreover, comprehensive understanding the detailed structural evolution of boehmite nanoparticles, the precursor of γ-alumina, certainly provide insight into the performance of the alumina, and open up new opportunities for their applications.

Acknowledgements

Financial Support from the Australian Research Council (ARC) and the NSFC of China (90206043) are gratefully acknowledged. HYZ is indebted to the ARC for a QE II Fellowship.

References

1. K.P. Goodboy, K.C. Dowing, in: L.D. Hart, E. Lense (Eds.), *Alumina Chemicals: Science and Technology Handbook* The American Ceramic Society Inc., Westervill, OH. 1990; p. 93.
2. C. Misra, *Industrial Alumina Chemicals*, ACS Monograph 184, American Chemical Society, Washington D. C., 1986, Chapter 2.
3. D.L. Trim, A. Stanislaus, Appl. Catal. 21 (1986) 215.
4. A.P. Philipse, A-M. Nechifor, C. Pathmamanoharan, Langmuir, 10 (1994) 4451.

5. J. Sterte, J.E. Otterstedt, Mat. Res. Bull. 21 (1986) 1159.
6. R.D. Cortright, R.R. Davda, J.A. Dumesic, Nature 418 (2002) 964.
7. F. Vaudry, S. Khodabandeh, M.E. Davis, Chem. Mater. 8 (1996) 1451.
8. S.A. Bagshaw, T.J. Pinnavaia, Angew. Chem., Int. Ed. Engl. 35 (1996) 1102.
9. P. Yang, D. Zhao, D.I. Margolese, B.F. Chmelka, G.D. Stucky, Nature, 396 (1998) 152.
10. H.Y. Zhu, J.D. Riches, J.C. Barry, Chem. Mater. 14 (2002) 2086.
11. Z.R. Zhang, T.J. Pinnavaia, J. Am. Chem. Soc. 124 (2002) 12294.
12. G. Lukasic, T. Rivkin, F. Tepper, Filtr. Sep. 39 (2002) 16.
13. S. Liu, R.J. Wehmschulte, C.M. Burba, J. Mater. Chem. 13 (2003) 3107.
14. G. Gundiah, F.L. Deepak, A. Govindaraj, C.N.R. Rao, Topics in Catalysis, 24 (2003) 137.
15. L.M. Bronstein, D.M. Chernyshov, R. Karlinsey, J.W. Zwanziger, V.G. Matveeva, E.M. Sulman, G.N. Demidenko, H.-P. Hentze, M. Antonietti, Chem. Mater. 15 (2003) 2623.
16. Y.Z. Jin, Y.Q. Zhu, K. Brigatti, H.W. Kroto, D.R.M. Walton, Appl. Phys. A: Mater. Sci. & Proces. 77 (2003) 113.
17. H.C. Lee, H.J. Kim, S.H. Chung, K.H. Lee, H.C. Lee, J.S. Lee, J. Am. Chem. Soc. 125 (2003) 2882.
18. H.J. Kim, H.C. Lee, C.H. Rhee, S.H. Chung, H.C. Lee, K.H. Lee, J.S. Lee, J. Am. Chem. Soc. 125 (2003) 13354.
19. D. Kuang, Y. Fang, H. Liu, C. Frommen, D. Fenske, J. Mater. Chem. 13 (2003) 660.
20. R.W. Hicks, N.B. Castagnola, Z. Zhang, T.J. Pinnavaia, C. L. Marshall, Appl. Catal., A: General. 254 (2003) 311.
21. S. Liu, R. J. Wehmschulte, C. M. Burba, J. Mater. Chem. 13 (2003) 3107.
22. G. Buelna, Y. S. Lin, L. X. Liu, J. D. Litster, Ind. Eng. Chem. Res. 42 (2003) 442.
23. H.Y. Zhu, X.P. Gao, D.Y. Song, Y.Q. Bai, S.P. Ringer, Z. Gao, Y.X. Xi, W. Martens, J.D. Riches, R.L. Frost, J. Phys. Chem. B 108 (2004) 4245.
24. O. Ozuna, G.A. Hirata, J. McKittrick, J. Phys. Cond. Matt. 16 (2004) 2585.
25. M. Linnolahti, T. A. Pakkanen, Inorg. Chem. 43 (2004) 1184.
26. H.C. Lee, H.J. Kim, C.H. Rhee, K.H. Lee, J.S. Lee, S.H. Chung, Micro. Meso. Mater. 79 (2005) 61.
27. M.L. Steigerwald, L.E. Brus, Accou. Chem. Res. 23 (1990) 183.
28. S.J. Gregg, K.S.W. Sing, Adsorption, Surface Area and Porosity, 2nd ed. Academic Press, New York, 1982.
29. H.Y. Zhu, P. Cool, E.F. Vansant, B.L. Su, X.P. Gao, Langmuir 20 (2004), 10115.
30. P.G. Cummins, J.B. Hayter, J. Pemfold, E. Staples, Chem. Phys. Lett. 138 (1987) 436.
31. P.G. Cummins, E. Staples, J. Pemfold, Langmuir, 5 (1989) 1195.
32. J. Pemfold, E. Staples, P.G. Cummins, Adv. Colloid Interface Sci. 34 (1991) 451.
33. Z. Lin, L.E. Scriven, H.T. Davis, Langmuir, 8 (1992) 2200.
34. W.-J. Li, E.-W.; Shi, W.-Z. Zhong, Z.-W. Yin, J. Cryst. Growth, 203 (1999) 186.
35. W. N. Martens, J. T. Kloprogge, R. L. Frost, J. R. Bartlett, J. Colloid Interf. Sci. 247 (2002) 132.
36. L.M. Bronstein, D.M. Chernyshov, R. Karlinsey. J.W. Zwanziger, V.G. Matveeva, E.M. Sulman, G.N. Demidenko, H.-P. Hentze, M. Antonietti, Chem. Mater. 15 (2003) 2623.

37. S. Mann, Nature, 365 (1993) 499.

LEGEND

Figure 1 TEM images of nanoparticulates obtained from the acidic reaction mixtures (pH<4) at different hydrothermal temperatures. (a) nanofibers prepared at 373K, (b) narrow porous laths prepared at 423K, (c) slit-like rings observed in the sample prepared at 423K and (d) the HRTEM image of wide porous laths prepared at 473K.

Figure 2 X-ray diffraction (XRD) patterns of the samples obtained at different temperatures. *a*) the patterns of samples obtained from the acidic reaction mixtures. *b*) and *c*) are the patterns of the samples prepared from neutral (pH ~6) and basic (pH >9) reaction mixtures, respectively. The bayerite phase is found in the sample prepared at 373K and pH > 9 and rest of the samples are boehmite crystals.

Figure 3 PSD of the porous nanolath samples (trace *a* is for the sample in Figure 1b and trace *b* for the one in Figure 1d), derived from N_2 adsorption data.

Figure 4 The TEM image (a) of porous γ-alumina laths obtained by heating the sample in image Fig 1b at 723K for 5 h. (b) is the XRD pattern of the γ-alumina laths.

Figure 5 The plot of ln *W* versus the reciprocal of temperature (1/*T*). *W* can also be regarded as the growth rate of the 1D-particulates in the direction of width.

Figure 6 HRTEM images of porous laths (a) and plates (b) in the products obtained at 473K, but pH <4 and pH >9, respectively.

Figure 7 TEM image of the porous laths prepared at 473K, pH <4. Most of the laths have two opposite sharp ends.

Figure 8 TEM image of the sample prepared at pH ~ 6, 473K. It is a mixture of porous laths and plates.

Figure 9 TEM image of stringy lath-shaped nanoparticulates of boehmite prepared with a PEG surfactant, instead of the PEO. There are no pores on the laths.

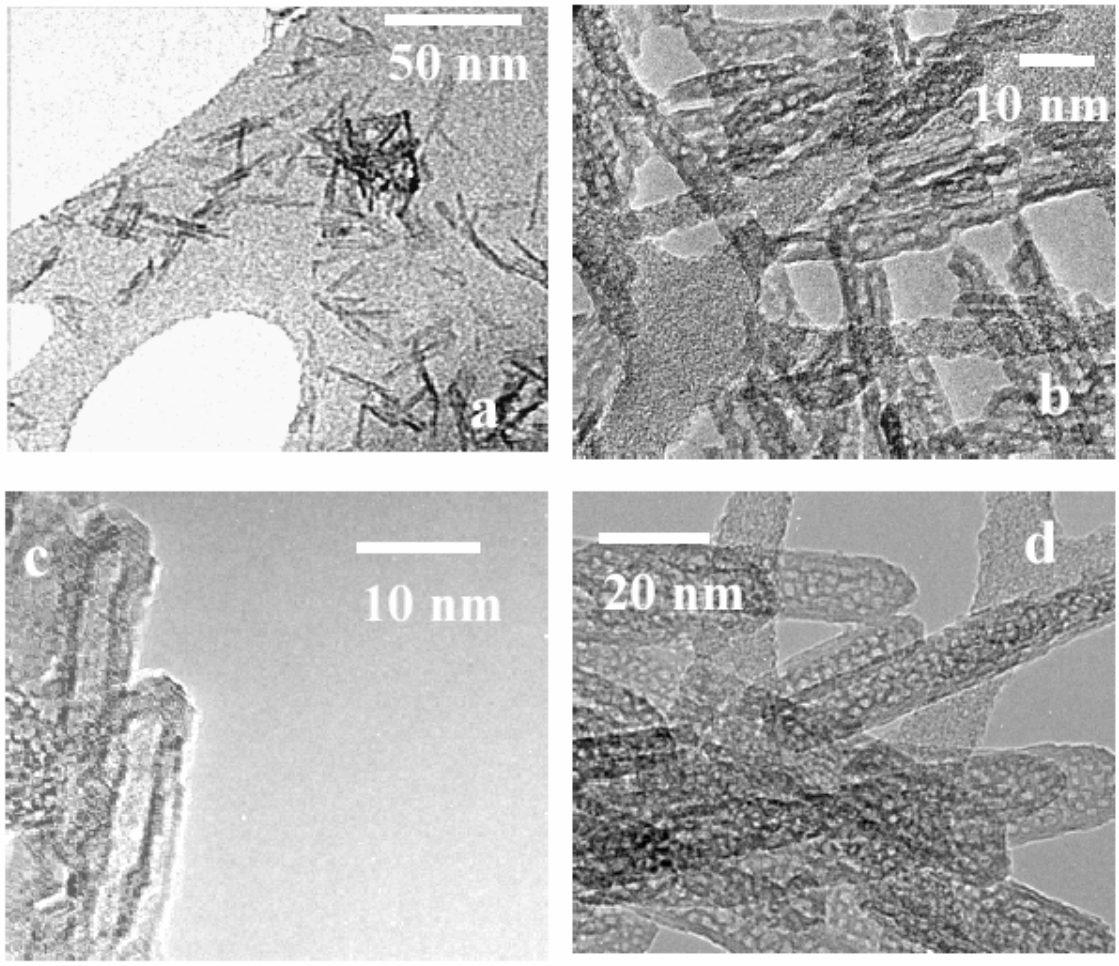

Figure 1

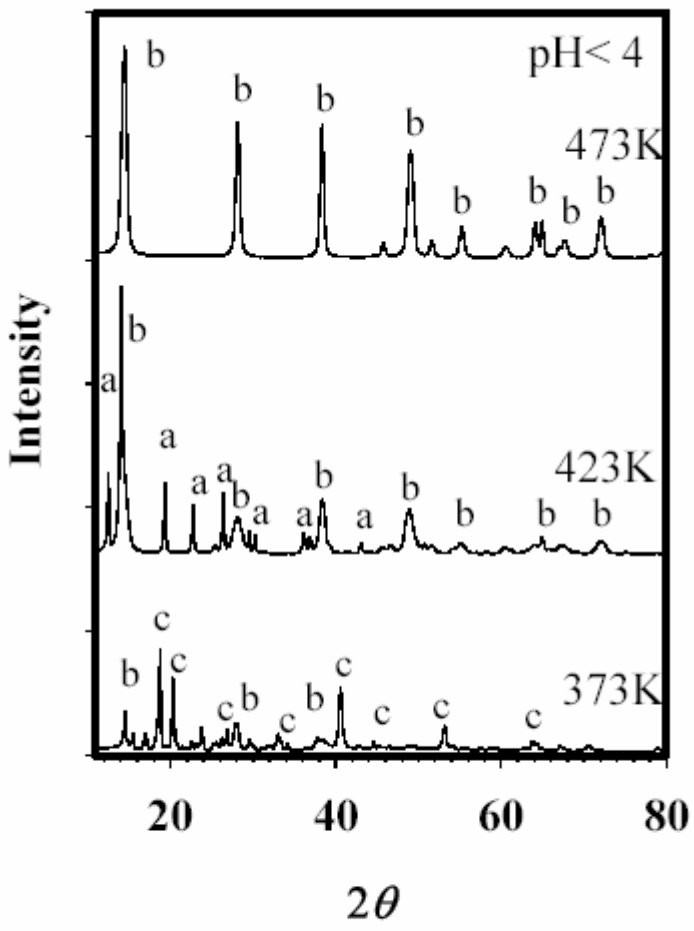

Figure 2a

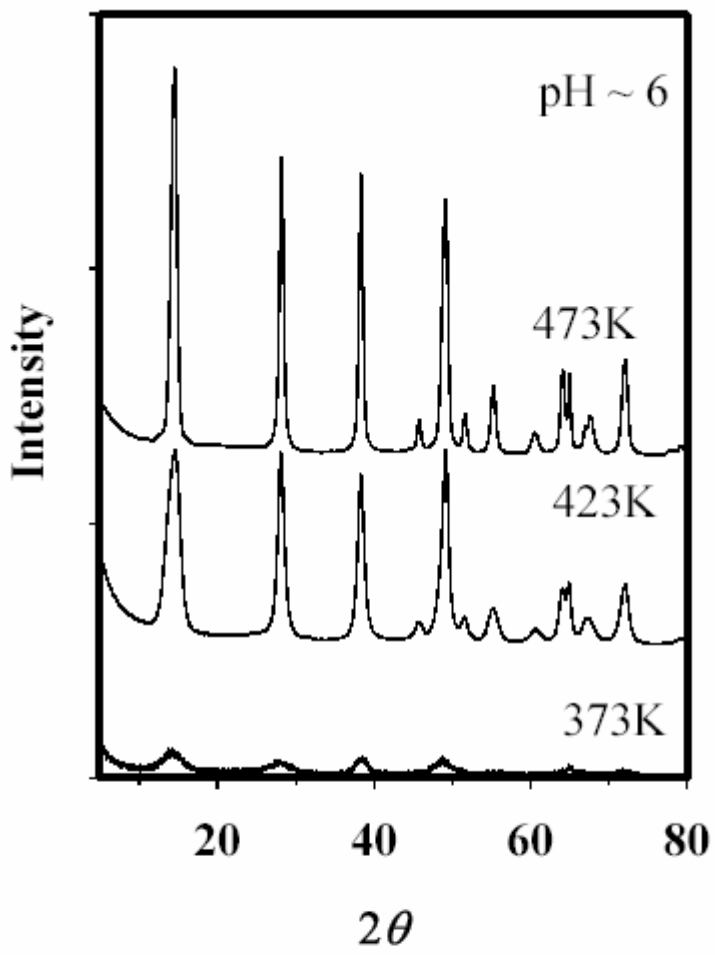

Figure 2b

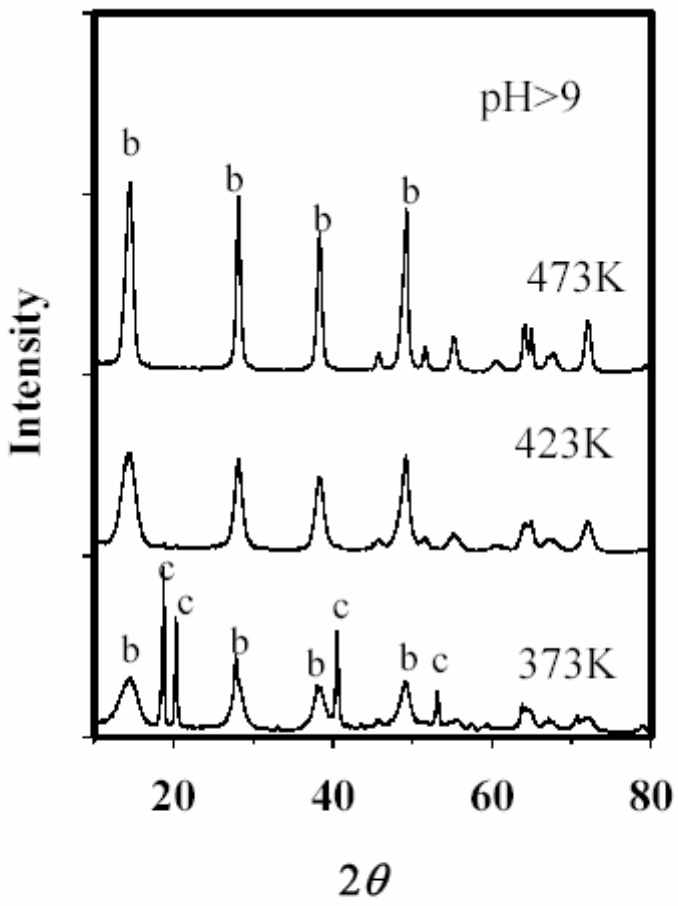

Figure 2c

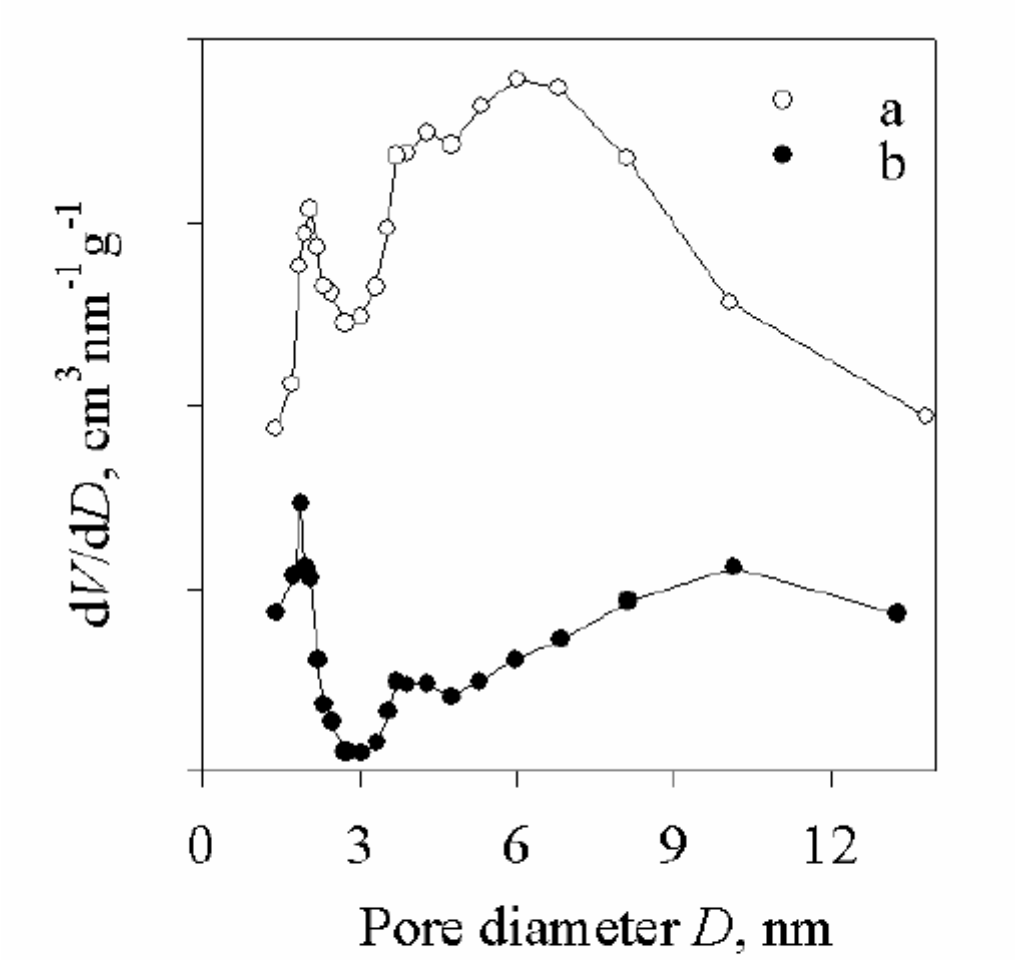

Figure 3

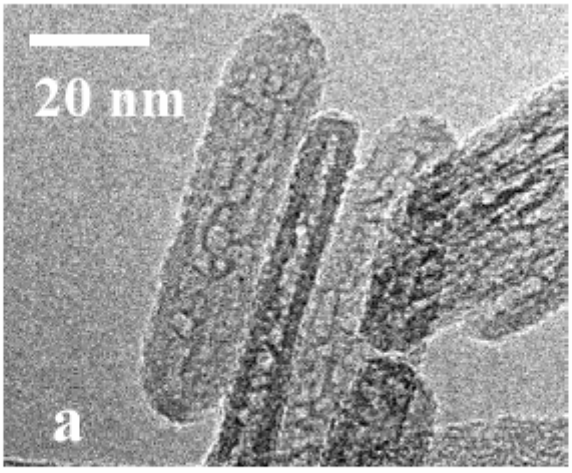

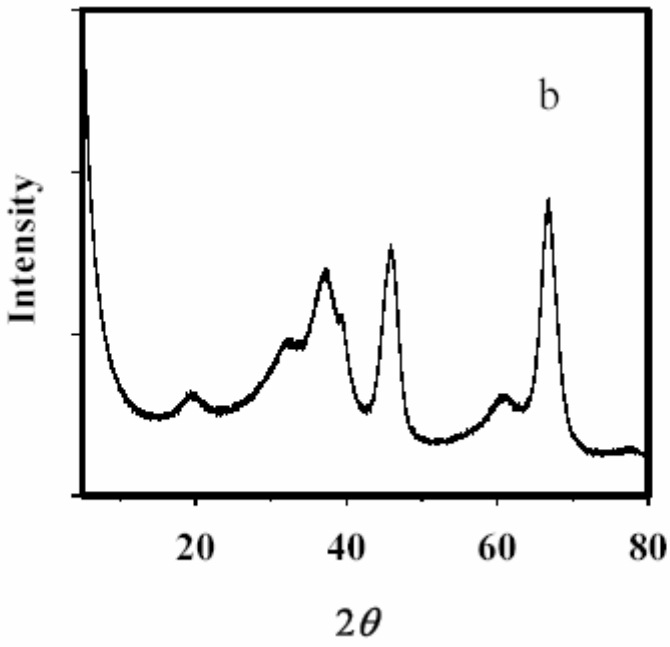

Figure 4

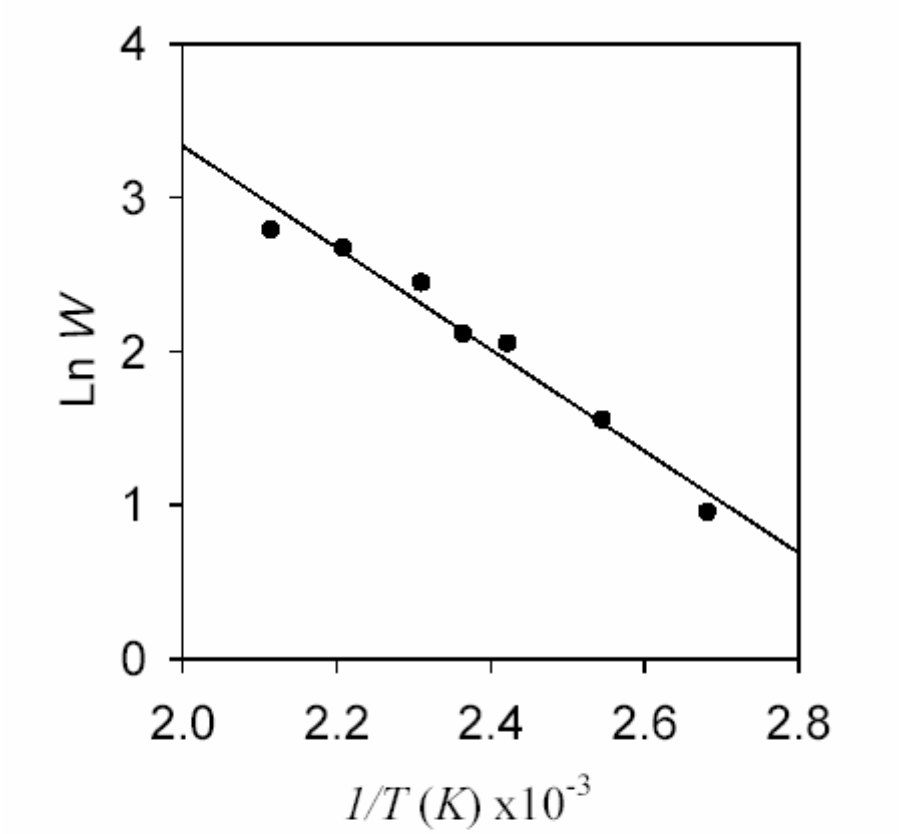

Figure 5

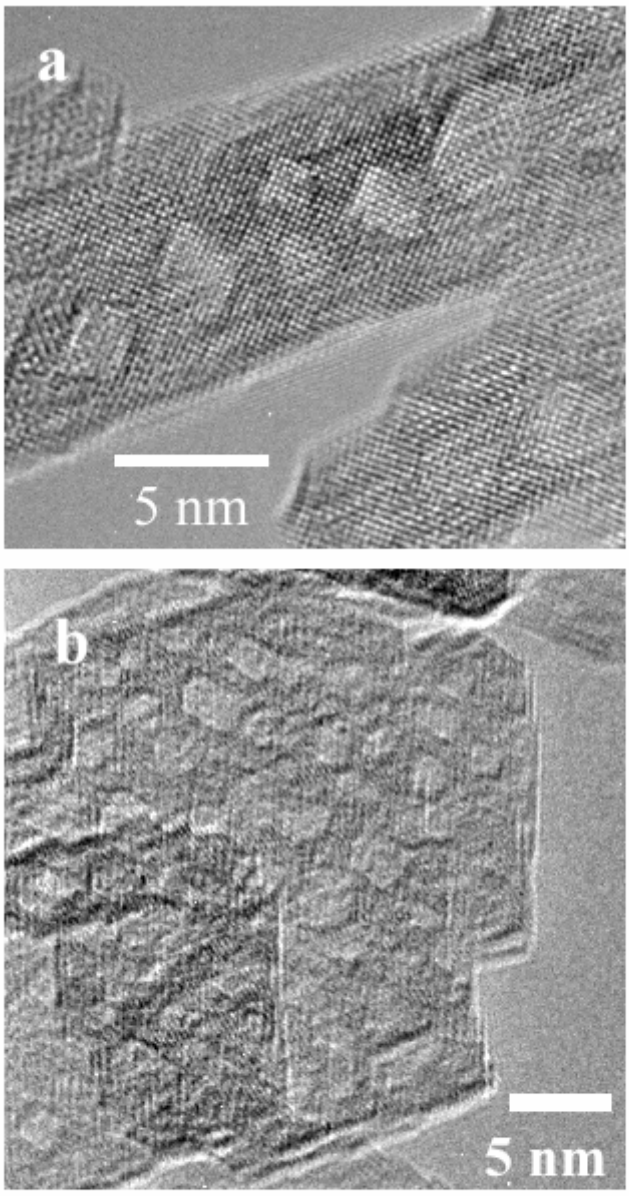

Figure 6

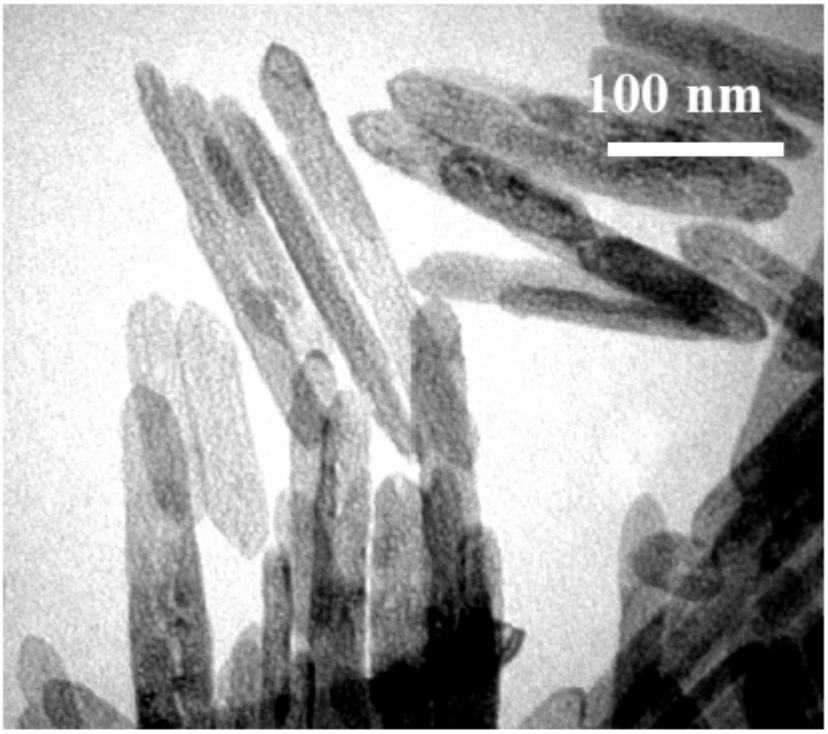

Figure 7

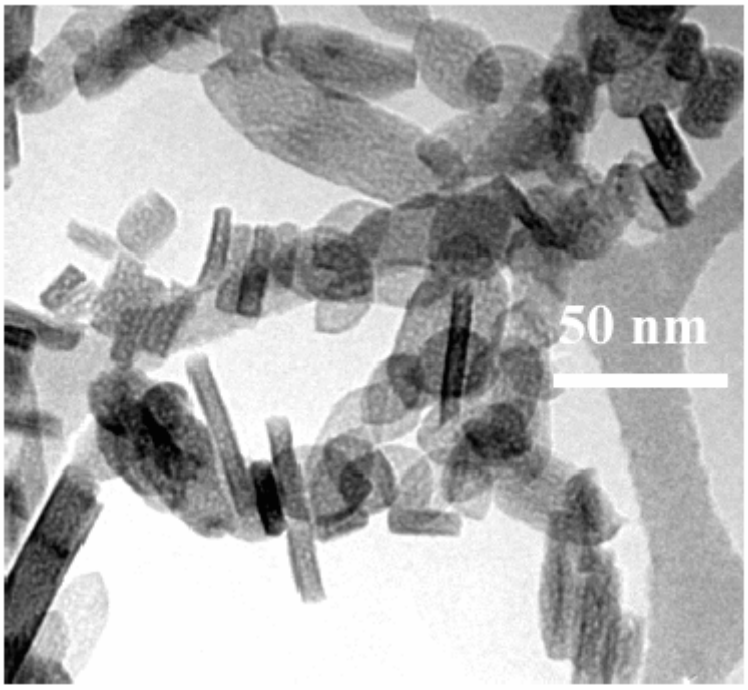

Figure 8

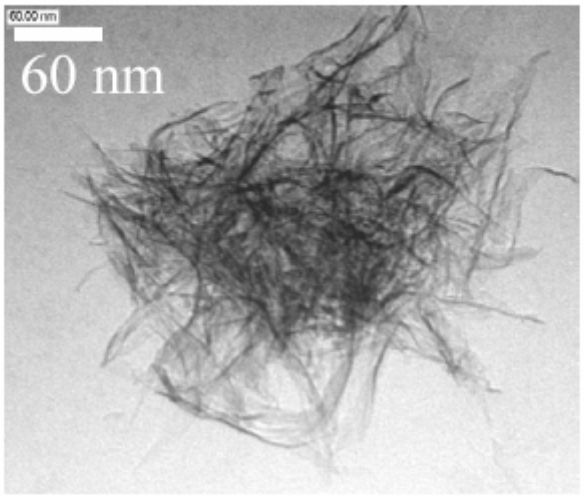

Figure 9